RESEARCH PAPER

Synthesis of worm-shaped carbon nanofibers over a sodium chloride support

R. Ravindra · Badekai Ramachandra Bhat

Abstract Worm-shaped carbon nanofibers (WCNFs) were synthesized in bulk by chemical vapour deposition at 680 °C using iron carboxylate as catalyst precursors and sodium chloride as catalyst support. The products were characterized by scanning electron microscopy, transmission electron microscopy, Raman spectroscopy and X-ray diffraction method. The purity of the purified products was determined by thermal analysis. The WCNF yield was 6700% relative to catalyst. The simplicity, environmental friendliness and use of easily available low-cost precursors are the advantage of this synthesis technique.

Keywords Worm-shaped carbon nanofibers · Chemical vapor deposition · Sodium chloride support · Iron carboxylates

Introduction

Since the discovery of carbon nanotubes (CNTs) in 1991 (Iijima), the research in the synthesis of carbon nanofibers (CNFs) and CNTs has been growing explosively because of their exciting physico-chemical, electrical and mechanical properties. CNTs and CNFs have large number of potential applications which include field emission sources (Milne et al. 2004), hydrogen storage (Dillon et al. 1997), catalyst substrate (Bahome et al. 2005), chemical sensors (Douglas and Alexander 2010), scanning probe tip (Demicheva et al. 2008), electrode material (Jan et al. 2009), nanoelectronics (Brataas 2008) and mechanical reinforcements (Wang et al. 2010). Among the synthetic methods, chemical vapour deposition (CVD) method has advantages of high yield, high selectivity and low-cost over traditional physical ones such as laser ablation and arc-discharge. The essential factors for the production of carbon nanomaterials by the CVD method are the catalyst system and carbon-source molecules. The catalyst is usually supported on insoluble alumina or silica substrate. The detrimental effect on the quality of the nano carbons is shown when strong acids are used to remove the substrates and catalyst during purification process (Schwarz et al. 1995). The catalytic growth of CNFs and CNTs has been explained based on vapour–liquid–solid (VLS) model. The VLS model consists of the following steps: (i) a carbon source is decomposed on the surface of transition metal nanoparticles (ii) liquidised metal carbide is formed by diffusion of carbon atoms into the nanoparticles (iii) after over saturation; the carbon precipitates to form CNFs or CNTs.

The carbon nanospecies of different shapes and morphologies are of great interest, because of their unique properties (Qi et al. 2010a). Helical CNFs and carbon nanocoils have their own applications in the

R. Ravindra · B. R. Bhat (✉)
Catalysis and Materials Laboratory, Department of Chemistry, National Institute of Technology Karnataka, Surathkal, Mangalore, 575 025, Karnataka, India
e-mail: chandpoorna@yahoo.com

field of composites (Yoshimura et al. 2006), hydrogen absorption (Furuya et al. 2004), as nanosprings (Chen et al. 2003) and as mass sensors (Volodin et al. 2004) because of their shape and unique characteristics. Recently the worm-shaped carbon nanotubes were synthesized and there magnetic properties were studied (Qi et al. 2010b) and Y-shaped CNFs were also synthesized by using ethanol flames (Cheng et al. 2008). Panchakarla et al. (2007) successfully synthesized worm-shaped carbon structures by using ruthenocene as catalyst precursor and ethylene as carbon source.

In this study, we propose a novel approach to synthesize worm-shaped carbon nanofibers (WCNFs) on water soluble support with iron carboxylate as catalyst precursors. Thermolysis of iron carboxylate in an argon atmosphere produces iron nanoparticles directly without using any calcination or reduction. Here, we report 6700% yield of WCNFs. High yield, simplicity and use of easily available low-cost precursors are the advantages of this route.

Experimental

WCNFs were synthesised by using iron-acetate, -formate and -oxalate as catalyst precursors. The supported catalysts were prepared by dispersing iron carboxylate on NaCl powder. The obtained supported catalysts were denoted as Fe acetate/NaCl, Fe formate/NaCl and Fe oxalate/NaCl. The WCNFs were grown using the CVD technique. Preparation of WCNFs was carried out in quartz tube of inner diameter 25 mm and length 90 mm. 300 mg of catalyst precursor with support was taken in quartz boat. The boat was placed in the centre of the quartz tube after the reactor reaches the desired temperature in an Argon atmosphere. On introduction of the acetylene gas, WCNF growth occurred. The CVD reaction was performed by passing a mixture of 1:10 C_2H_2:Ar for 15 min at 680 °C. In an argon atmosphere, the reaction was allowed to cool to room temperature and obtained black product was collected. The carbon yield is calculated by Eq. 1:

$$\frac{M_{\text{Total}} - M_{\text{Cat}}}{M_{\text{Cat}}} \times 100 = \text{Carbon yield}\% \quad (1)$$

where M_{Total} is the total mass of the carbon product and catalyst, and M_{Cat} is the mass of the catalyst.

To purify the sample, the raw material was first heated under an air atmosphere at 380 °C for 2 h to ensure complete removal of amorphous carbon and then stirred in warm water to remove the catalyst and sodium chloride support. The sample was finally washed with deionized water and dried in vacuum oven.

Nanostructure and morphology of WCNF were observed under both scanning electron microscope (SEM, SUPRA 40VP Carl Zeiss) and transmission electron microscope (TEM, CM200 Philips). The purity and structural stability of WCNF was determined by the Thermogravimetric analysis (TGA). The TGA was performed on SDT Q600 (TA, USA) using dry air as the carrier gas (flow rate: 50 mL/min). A Raman spectrum was used to understand the relative intensity of G- and D-band (Renishaw, RM 1000, He–Ne laser excitation line at 633.0 nm) at ambient condition. The X-ray diffraction (XRD) patterns were obtained (JEOL JDX 8P diffractometer with Cu Kα radiation, $\lambda = 1.5418$ Å) to determine WCNF purity and crystallinity.

Results and discussion

In an inert gas flow system, metal carboxylate catalyst precursors decompose directly into metallic nanoparticles without forming the oxide intermediate (Edwards et al. 1997; Jesus et al. 2005). Thus, this method of synthesizing nanoparticles as catalyst for the growth of carbon nanostructures has advantages over other inorganic salts like metal nitrates or oxides. The lengthy process of calcination and reduction for the preparation of catalyst is eliminated as metal carboxylate precursors directly yield metal nanoparticles (Kathyayini et al. 2008). The support used for catalysts is sodium chloride, which is easily soluble in water. So the problems such as detrimental effect, environment and even cost has been overcome by using sodium chloride as support. Table 1 gives summary of catalyst precursor, wt% of metal in support, CVD parameters and I_D/I_G ratio of WCNFs produced.
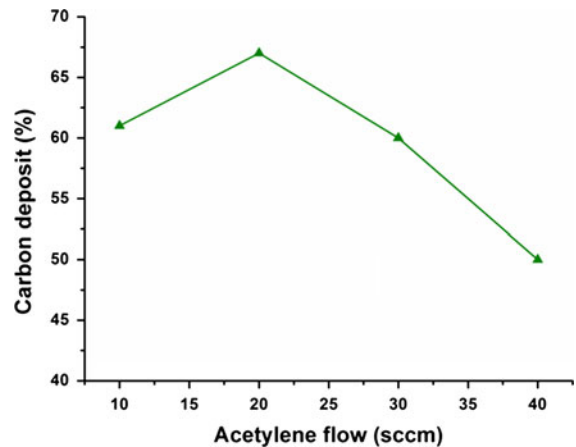
The effect of reaction temperature on the yield of carbon deposits were studied for the iron formate catalyst precursor. The melting point of NaCl is 760 °C, so all reactions were performed within this temperature. At reaction temperatures between 600 and 740 °C, a variety of experiments were done with

Table 1 Summary of catalyst precursor, wt% of metal in support, CVD parameters and I_D/I_G ratio of WCNFs produced

Catalyst precursor on NaCl support	Wt% of metal in support	Gas flow rate (sccm) Temperature	I_D/I_G ratio
Iron acetate	3	$C_2H_2 = 20$ Ar $= 200$ 680 °C	$I_D/I_G = 1.11$
Iron formate	3	$C_2H_2 = 20$ Ar $= 200$ 680 °C	$I_D/I_G = 1.05$
Iron oxalate	3	$C_2H_2 = 20$ Ar $= 200$ 680 °C	$I_D/I_G = 1.23$
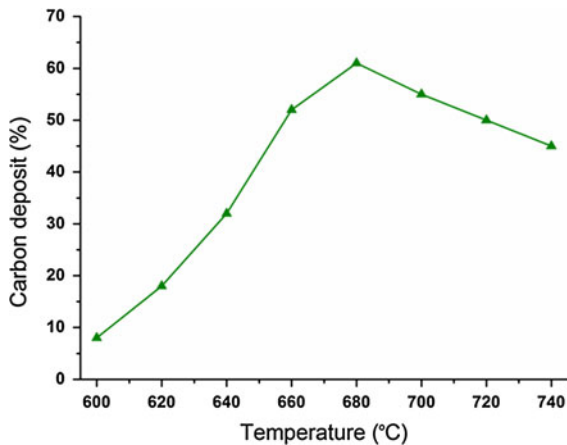
Fig. 1 Amount of carbon deposit with different temperature at gas flow (10 sccm C_2H_2: 200 sccm Ar) for iron formate catalyst precursor

Fig. 2 Amount of carbon deposit with different gas flow of acetylene (sccm), at constant flow of 200 sccm of Argon at 680 °C for iron formate catalyst precursor

acetylene–argon mixture (10 sccm:200 sccm) (Fig. 1). The carbon deposit was maximum at 680 °C. The increase of carbon yield with increasing temperature till 680 °C was due to the enhanced diffusion of carbons into metal catalyst and decrease in the carbon yield after 680 °C may be due to softening of support and hence interaction between metal catalyst and carbon becomes lesser. Further, the effects of acetylene flow rate on the carbon deposits were studied and the results are presented in Fig. 2. At 680 °C, the reactions were performed at various volumes of acetylene for 15 min. When the flow rate was increased from 10 to 20 sccm, we observed an increase in the carbon deposit, and then the percentage of carbon deposit was decreased when the flow rate was increased to 30 sccm. This is because the rate of diffusion of carbon into catalyst particle was slower than that of acetylene decomposition, which would have resulted in the formation of amorphous carbon and deactivates the

catalyst. So all the reactions were performed at 680 °C with gas flow of 200 sccm:20 sccm (Ar:C_2H_2) for 15 min. The metal loading percentage was fixed to 3 wt% in support in order to avoid sintering effect of catalyst at high temperatures.

Representative SEM and TEM images of the purified WCNF grown on iron acetate/NaCl, iron formate/NaCl and iron oxalate/NaCl are shown in Figs. 3 and 4. As can be seen there is a clear evidence for the production of high purity WCNF, and the catalytic particles and amorphous carbon were removed successfully by the purification. Because of their twisting morphology it is difficult to measure the length of the WCNF from the SEM micrographs, but the length can be estimated to be more than several tens of micrometers. The WCNF were further characterised by using TEM. The TEM images assure that nanostructures formed are CNFs. The average diameters of CNFs are in the range of 20–60 nm (Fig. 4).
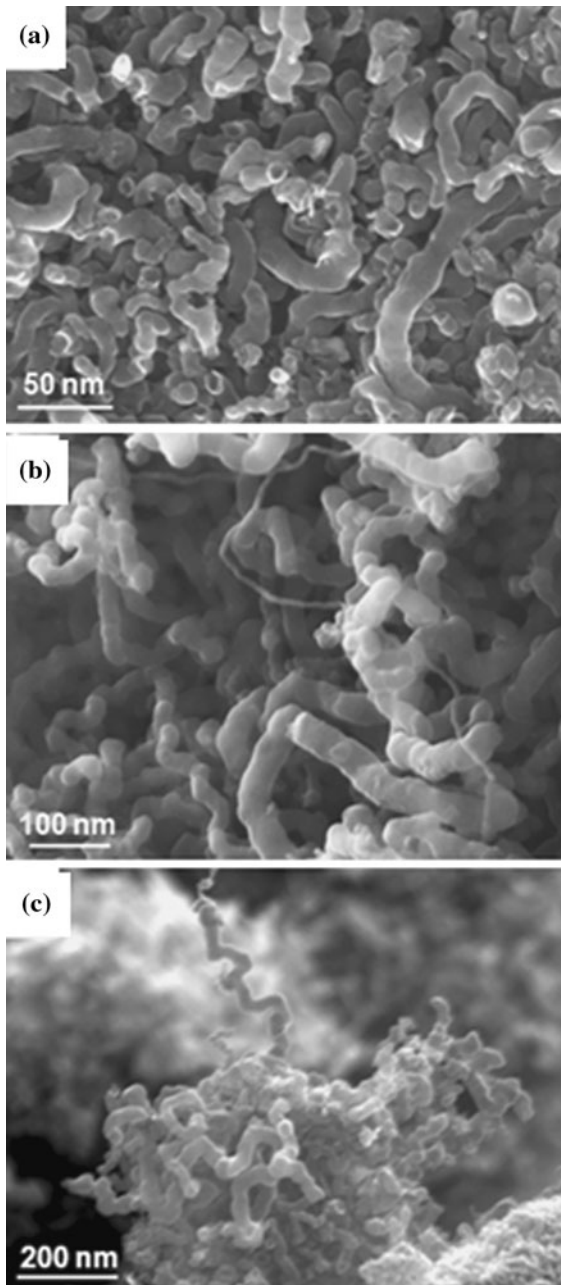
Fig. 3 SEM images of purified WCNFs grown on **a** iron acetate, **b** iron formate, **c** iron oxalate as catalyst precursors

Fig. 4 TEM images of purified WCNFs grown on **a** iron acetate, **b** iron formate, **c** iron oxalate as catalyst precursors

Raman spectroscopy is a useful technique to analyze the degree of graphitization of WCNF. It provides information about the crystal structure and the presence of the disorder and defects. The Raman spectra of the purified WCNF samples are shown in Fig. 5. It can be seen that spectra of all samples consist of two peaks: the peak of C–C stretching mode
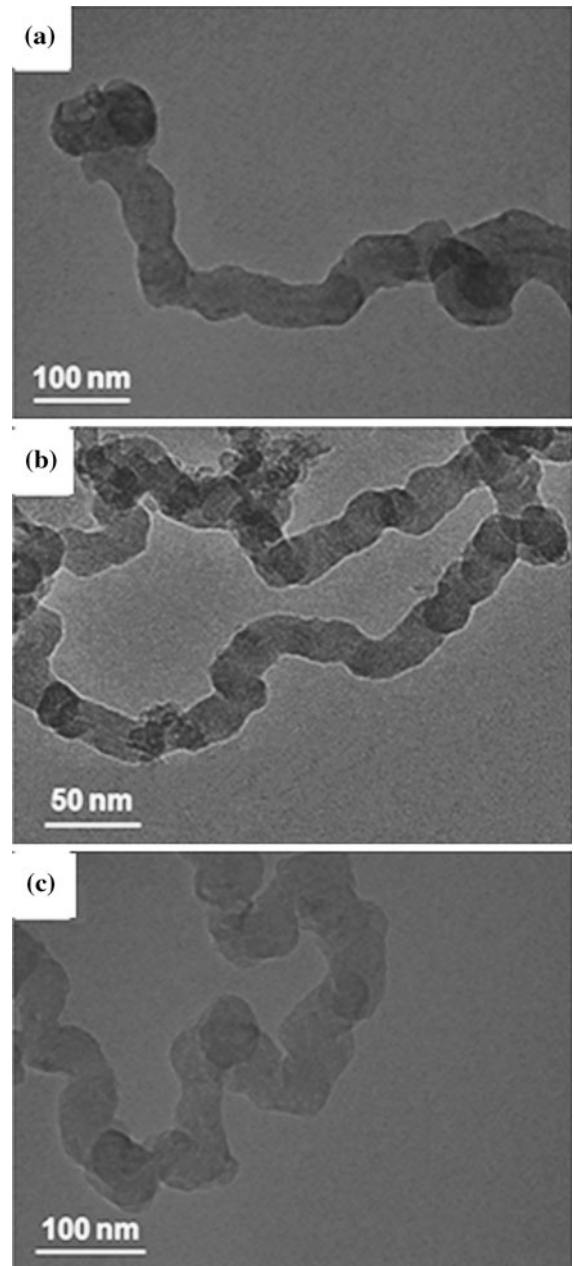
(G-band) appeared at around 1,590 cm^{-1}, which indicates the presence of graphene layers in WCNFs. D-band at around 1,330 cm^{-1} indicates the existence of defective graphene layers. The ratio I_D/I_G of intensities of the D- and G-bands is regarded as an index for the crystalline order of CNFs. A lower I_D/I_G value indicates a higher degree of graphitization.
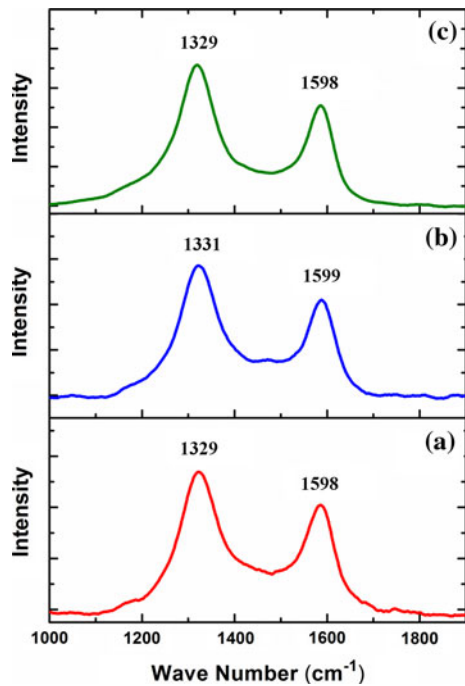
Fig. 5 Raman spectra of purified WCNFs grown on **a** iron acetate, **b** iron formate, **c** iron oxalate as catalyst precursors
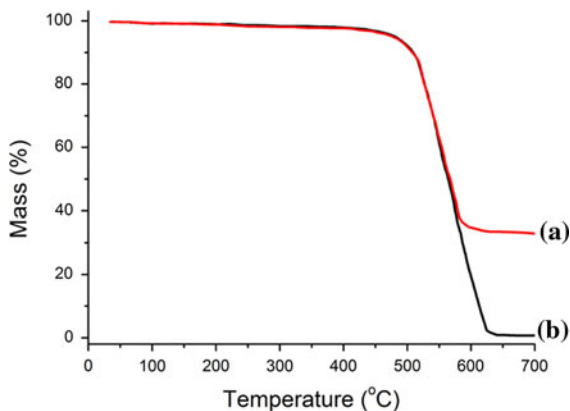

Fig. 7 XRD pattern of purified WCNFs grown on (*a*) iron acetate (*b*) iron formate (*c*) iron oxalate as catalyst precursors

Fig. 6 TGA analysis of carbon products grown on (**a**) iron formate (**b**) purified product grown on iron formate

The I_D/I_G value for purified WCNFs grown is almost unity, indicating presence of lesser defects.

Thermogravimetric analysis is a useful technique to estimate the purity of WCNF. The weight loss profile in Fig. 6 was obtained by heating the as grown and purified WCNF from room temperature to 700 °C at a rate of 10 °C/min in air atmosphere. TGA analysis of product obtained over iron formate showed no we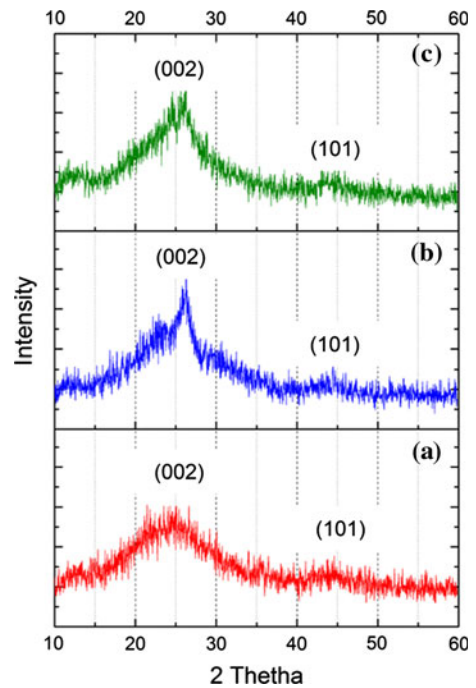ight loss in air until 470 °C; this indicates the absence of amorphous carbon. The main loss at ∼520 °C indicates that WCNF are stable till 500 °C. The analysis revealed that after the purification, the purity of WCNF product was better than 98.5%.

The purified samples were also characterized by using XRD diffractometer. The XRD pattern (Fig. 7) also shows the structural feature of WCNF. The spectra contains two characteristic peaks at 26.0° and 43.5°, indexed with (002) and (101) diffraction planes of hexagonal graphite (JCPDS card files, no. 41-1487), respectively. No other noticeable peaks induced by catalyst or support can be observed in the XRD pattern.

Conclusions

Thus, we proposed a simple route to synthesize WCNFs in an economical and environmental friendly way. Iron carboxylates directly yield iron nanoparticles on pyrolysis, thereby eliminating the lengthy process of calcination and reduction. Sodium chloride was used as support because of its water solubility and non-toxicity nature. In particular, the WCNF yield

obtained by iron formate, iron acetate and iron oxalate were almost same. This method is a simple, environment friendly and low-cost approach for mass production of WCNFs.

References

Bahome MC, Jewell LL, Padayachy K, Hildebrandt D, Glasser D, Datye AK, Coville NJ (2005) Fischer–Tropsch synthesis over iron catalysts supported on carbon nanotubes. Appl Catal A 287:60–67

Brataas A (2008) Nanoelectronics: spin surprise in carbon. Nature 452:419–420

Chen XQ, Zhang SL, Dikin DA, Ding WQ, Ruoff RS, Pan LJ (2003) Mechanics of carbon nanocoils. Nano Lett 3:1299–1304

Cheng J, Zou X, Zhang H, Li F, Ren P, Zhu G, Su Y, Wang M (2008) Growth of Y-shaped carbon nanofibers from ethanol flames. Nanoscale Res Lett 3:295–298

Demicheva OV, Meshkov GB, Sinitsyna OV, Tomishko AG, Yaminsky IV (2008) Multiwall carbon nanotube tips for scanning probe microscopy. Nanotechnol Russ 3:704–709

Dillon AC, Jones KM, Bekkedahl TA, Kiang CH, Bethune DS, Heben MJ (1997) Storage of hydrogen in single-walled carbon nanotubes. Nature 386:377–379

Douglas RK, Alexander S (2010) Graphene versus carbon nanotubes for chemical sensor and fuel cell applications. Analyst 135:2790–2797

Edwards AB, Garner CD, Roberts KJ (1997) In situ QXAFS study of the pyrolytic decomposition of nickel formate dihydrate. J Phys Chem B 101:20–26

Furuya Y, Hashishin T, Iwanaga H, Motojima S, Hishikawa Y (2004) Interaction of hydrogen with carbon coils at low temperature. Carbon 42:331–335

Iijima S (1991) Helical microtubules of graphitic. Carbon 354:56–58

Jan E, Hendricks JL, Husaini L, Burns SMR, Sereno A, Martin DC, Kotov NA (2009) Layered carbon nanotube-polyelectrolyte electrodes outperform traditional neural interface materials. Nano Lett 9:4012–4018

Jesus JCD, Gonzalez I, Quevedo A, Puerta T (2005) Thermal decomposition of nickel acetate tetrahydrate: an integrated study by TGA, QMS and XPS techniques. J Mol Catal A: Chem 288:283–291

Kathyayini H, Reddy KV, Nagy JB, Nagaraju N (2008) Synthesis of carbon nanotubes over transition metal ions supported on Al(OH)$_3$. Indian J Chem (Sec B) 47A:663

Milne WI, Teo KBK, Amaratunga GAJ, Legagneux P, Gangloff L, Schnell JP, Semet V, Thien VB, Groening O (2004) Carbon nanotubes as field emission sources. J Mater Chem 14:933–943

Panchakarla LS, Govindaraj A (2007) Carbon nanostructures and graphite-coated metal nanostructures obtained by pyrolysis of ruthenocene and ruthenocene–ferrocene mixtures. Bull Mater Sci 30:23

Qi X, Qin C, Zhong W, Au C, Ye X, Du Y (2010a) Large-scale synthesis of carbon NanoMaterials by catalytic chemical vapor deposition: a review of the effects of synthesis parameters and magnetic properties. Materials 3:4142–4174

Qi X, Zhong W, Deng Y, Au C, Du Y (2010b) Synthesis of helical carbon nanotubes, worm-like carbon nanotubes and nanocoils at 450 °C and their magnetic properties. Carbon 48:365–376

Schwarz JA, Contescu C, Contescu A (1995) Methods for preparation of catalytic materials. Chem Rev 95:477–510

Volodin A, Buntinx D, Ahlskog M, Fonseca A, Nagy JB, Haesendonck CV (2004) Coiled carbon nanotubes as self-sensing mechanical resonators. Nano Lett 4:1775–1779

Wang Y, Shi Z, Yin J (2010) Unzipped multiwalled carbon nanotubes for mechanical reinforcement of polymer composites. J Phys Chem C 114:19621

Yoshimura K, Nakano K, Miyake T, Hishikawa Y, Motojima S (2006) Effectiveness of carbon microcoils as a reinforcing material for a polymer matrix. Carbon 44:2833–2838